Nonperturbative Effects of Energetic Ions on Alfvén Eigenmodes

Y. Todo 1), N. Nakajima 1), K. Shinohara 2), M. Takechi 2), M. Ishikawa 2), S. Yamamoto 3)

1) National Institute for Fusion Science, Toki, Japan
2) Naka Fusion Research Establishment, Japan Atomic Energy Research Institute, Naka, Japan
3) Institute of Advanced Energy, Kyoto University, Uji, Japan

e-mail contact of main author: todo@nifs.ac.jp

Abstract. Linear properties and nonlinear evolutions of an energetic-ion driven instability in a JT-60U plasma were investigated using a simulation code for magnetohydrodynamics and energetic particles. The spatial profile of the unstable mode peaks near the plasma center where the safety factor profile is flat. The unstable mode is not a toroidal Alfvén eigenmode (TAE) because the spatial profile deviates from the expected location of TAE and the spatial profile consists of a single primary harmonic $m/n = 2/1$ where m, n are poloidal and toroidal mode numbers. The real frequency of the unstable mode is close to the experimental starting frequency of the fast frequency sweeping mode. The simulation results demonstrate that the energetic ion orbit width and the energetic ion pressure significantly broaden radial profile of the unstable mode. For the smallest value among the investigated energetic ion orbit width, the unstable mode is localized within 20% of the minor radius. This gives an upper limit of the spatial profile width of the unstable mode which the magnetohydrodynamic effects alone can induce. For the experimental condition of the JT-60U plasma, the energetic ions broaden the spatial profile of the unstable mode by a factor of 3 compared with the smallest orbit width case. The unstable mode is primarily induced by the energetic particles. It is demonstrated that the frequency shifts both upward and downward in the nonlinear evolution at the rate close to that of the fast frequency sweeping mode. In addition to the energetic particle mode in the JT-60U plasma, an investigation of TAE in an LHD-like plasma using the simulation code for the helical coordinate system is reported.

1. Introduction

Three types of frequency chirping instabilities, slow frequency sweeping (slow FS) mode, fast frequency sweeping (fast FS) mode, and abrupt large event (ALE) have been observed in the JT-60U plasmas heated with negative ion based neutral beam (NNB) injection [1, 2, 3, 4]. The frequencies of the three instabilities are in the range of shear Alfvén eigenmodes. The frequency sweeping of the slow FS mode has a good correlation with the equilibrium parameter evolution with a time scale $\simeq$200 ms. On the other hand, the time scales of the fast FS mode and the ALE are respectively 1-5 ms and 200-400 μs, much shorter than the equilibrium time scale. The frequency of the fast FS mode shifts rapidly by 10-20 kHz in 1-5ms both upward and downward. The starting frequency of the fast FS mode changes in the time scale of the equilibrium parameter evolution and follows the toroidal Alfvén eigenmode (TAE) [5, 6] gap frequency.

We have investigated the fast FS mode in a JT-60U plasma using a simulation code for magnetohydrodynamics (MHD) and energetic particles, MEGA [7]. We reported that there is an unstable mode near the plasma center and a frequency sweeping close to that of the fast FS mode takes place [8]. The ratio of the linear damping rate (γ_d) to the linear growth rate (γ_L) in the simulation is consistent with the hole-clump pair creation which takes place when γ_d/γ_L is greater than 0.4 [9, 10].

In Ref. [8], we called the unstable mode "nonlocal energetic particle mode (EPM)" and argued that it is different from the resonant type EPM [11, 12] and similar to the EPM which is predicted for ICRF heated plasma with reversed magnetic shear [13, 14]. However, it was shown numerically that the reversed-shear-induced Alfvén eigenmode (RSAE), which has properties similar to the global Alfvén eigenmode (GAE) [15], can exist in reversed shear plasmas [16]. In

Ref. [17] it is theoretically clarified that both toroidal MHD effects of second order in inverse aspect ratio and adiabatic response of energetic particles can establish an eigenmode localized near the magnetic surface where the safety factor takes the minimum value in reversed shear plasmas. This gives us a new viewpoint to investigate linear properties of the nonlocal EPM which we reported in Ref. [8]. We have carried out simulations for various energetic ion orbit widths and energetic ion pressures using the MEGA code and found that they have significant effects on the spatial profile of the unstable mode in the JT-60U plasma [18]. In this paper, we report the linear properties and the frequency sweeping of the nonlocal EPM in sections 3 and 4, repectively. The simulation model is described in section 2. Section 5 is devoted to an investigation of TAE in an LHD-like plasma using the simulation code for the helical coordinate system.

2. Simulation Model

The hybrid simulation model for MHD and energetic particles [19, 20, 7] is employed in the MEGA code. The plasma is divided into the bulk plasma and the energetic ions. The bulk plasma is described by the nonlinear full MHD equations. The electromagnetic field is given by the MHD description. This approximation is reasonable under the condition that the energetic ion density is much less than the bulk plasma density. The MHD equations with energetic ion effects are,

$$\frac{\partial \rho}{\partial t} = -\nabla \cdot (\rho \mathbf{v}), \tag{1}$$

$$\rho \frac{\partial}{\partial t}\mathbf{v} = -\rho \boldsymbol{\omega} \times \mathbf{v} - \rho \nabla (\frac{v^2}{2}) - \nabla p + (\mathbf{j} - \mathbf{j}_h) \times \mathbf{B} - \nu \rho \nabla \times \boldsymbol{\omega} + \frac{4}{3} \nu \rho \nabla (\nabla \cdot \mathbf{v}), \tag{2}$$

$$\frac{\partial \mathbf{B}}{\partial t} = -\nabla \times \mathbf{E}, \tag{3}$$

$$\frac{\partial p}{\partial t} = -\nabla \cdot (p\mathbf{v}) - (\gamma - 1) p \nabla \cdot \mathbf{v} + (\gamma - 1)[\nu \rho \omega^2 + \frac{4}{3} \nu \rho (\nabla \cdot \mathbf{v})^2 + \eta j^2], \tag{4}$$

$$\mathbf{E} = -\mathbf{v} \times \mathbf{B} + \eta \mathbf{j}, \tag{5}$$

$$\boldsymbol{\omega} = \nabla \times \mathbf{v}, \tag{6}$$

$$\mathbf{j} = \frac{1}{\mu_0} \nabla \times \mathbf{B}, \tag{7}$$

where μ_0 is the vacuum magnetic permeability and γ is the adiabatic constant, and all the other quantities are conventional. Here, $\mathbf{j}_h$ is the energetic ion current density without $\mathbf{E} \times \mathbf{B}$ drift.

The effect of the energetic ions on the MHD fluid is taken into account in the MHD momentum equation [Eq. (2)] through the energetic ion current. The MHD equations are solved using a finite difference scheme of fourth order accuracy in space and time. The drift-kinetic description is employed for the energetic ions. The δf method [21, 22, 23] is used for the energetic ions. The marker particles are initially loaded uniformly in the phase space. With the uniform loading employed in this work, the number of energetic beam ions that each marker particle represents is in proportion to the initial distribution function, namely the particle density in the phase space. It is important to start the simulation from the MHD equilibrium consistent with the energetic ion distribution. We solve an extended Grad-Shafranov equation developed in Ref. [24] in the cylindrical coordinates (R, φ, z) where R is the major radius coordinate, φ is the toroidal angle coordinate, and z is the vertical coordinate. The MEGA code is benchmarked with respect to the alpha-particle-driven $n = 4$ TAE in the TFTR D-T plasma shot #103101 [25]. The destabilized mode has a TAE spatial profile which consists of two major harmonics $m/n = 6, 7/4$ and frequency 215kHz. These results are consistent with the calculation with the NOVA-K code [26]. The linear growth rate obtained from this simulation, is 8.7×10^{-3} of

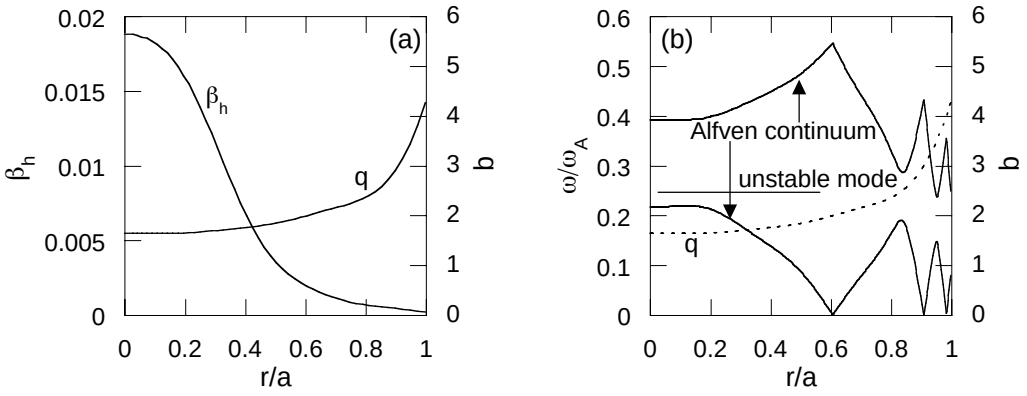

FIG. 1. Energetic ion beta (β_h) profile and safety factor (q) profile; (a). Frequency and location of the unstable mode with q-profile and the shear Alfvén continuous spectra with the toroidal mode number $n = 1$; (b).

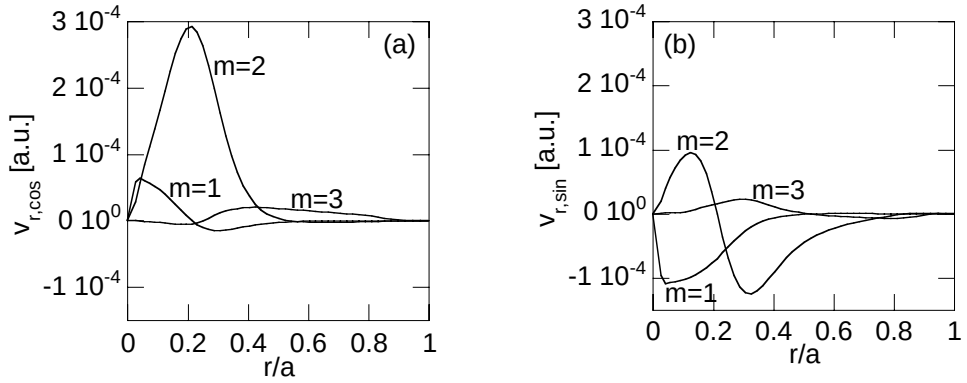

FIG. 2. Spatial profiles of (a) cosine part and (b) sine part of the unstable mode radial velocity v_r harmonics for $\rho_{h\|}/a = 0.08$. The toroidal mode number of all the harmonics is $n = 1$.

the mode frequency. This linear growth rate is close to what is observed in the previous particle simulation 1.1×10^{-2} [27] and calculated in the NOVA-K code 8×10^{-3} [26].

3. Nonlocal Energetic Particle Mode

3.1. Instability in a JT-60U Plasma

The JT-60U discharge E36379 [3], where the fast FS mode was observed, was investigated using the MEGA code. The safety factor profile, bulk pressure profile, and density profile used in the simulation are based on the experimental data. The major and minor radii are R_0 =3.4m and a=1.0m, respectively. The shape of the outermost magnetic surface in the simulation is circular while it was diverter-shaped in the experiment. The magnetic field at the magnetic axis is 1.2T. The bulk plasma and the beam ions are deuterium. The NNB injection energy is 346keV. The initial energetic ion distribution in the velocity space is assumed to be a slowing down distribution. The energetic ion velocity perpendicular to magnetic field is neglected because the NNB injection is tangential. The beam direction is parallel to the plasma current. The maximum velocity is assumed to be 80% of the injection velocity as the injection is not completely parallel to the magnetic field. This maximum velocity in the simulation corresponds roughly to the Alfvén velocity at the magnetic axis. The NNB injection and the collisions are neglected in the simulations in this paper. The number of marker particles used is 5.2×10^5. The numbers of

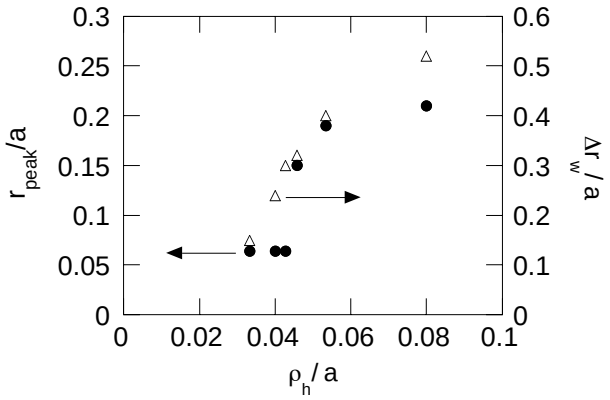

FIG. 3. Peak location (r_{peak}) and radial width (Δr_w) of the unstable mode spatial profile versus energetic ion parallel Larmor radius normalized by the minor radius.

grid points are $(101, 16, 101)$ for the cylindrical coordinates (R, φ, z).

A linearly unstable mode was investigated for energetic ion pressure profile based on a calculation using the OFMC code [28]. The OFMC code calculation gives classical distribution, which is established by the NNB injection and the particle collisions. Energetic ion redistributions and losses due to the ALE and the fast FS mode are not considered in the OFMC code calculation. The energetic ion pressure profile and q-profile used in the simulation are shown in Fig. 1(a). The central beta value is 1.9%. The ratio of energetic ion parallel Larmor radius, which is defined by the maximum parallel velocity and the Larmor frequency, to the minor radius $\rho_{h\|}/a$ is 0.08. An unstable mode was found in the TAE range of frequency. Figure 1(b) shows the frequency and the location of the unstable mode. The location of the unstable mode is defined by the region where the total intensity of sine and cosine parts of the $m/n = 2/1$ harmonic of radial velocity v_r is larger than 10% of the peak value. The frequency of the unstable mode is $0.25\omega_A$ where $\omega_A = v_A/R_0$ and v_A is the Alfvén velocity at the plasma center. The frequency corresponds to 52 kHz, which is close to the starting frequency of the fast FS mode. In Fig. 1(b) also shown are the $n = 1$ shear Alfvén continuous spectra. The gap in the Alfvén continuous spectra at $q = 2.5$ for $m/n = 2, 3/1$ harmonics is located at $r/a \sim 0.8$. If the unstable mode is a TAE, it must be located at the gap ($r/a \sim 0.8$) and must consist of two major harmonics. The unstable mode found in the simulation does not have the properties of TAE. Thus, we conclude it is not a TAE. The spatial profile of the radial velocity v_r of the unstable mode is shown in Fig. 2. The primary harmonic is $m/n = 2/1$, where m and n are the poloidal and toroidal mode numbers. Phases in all of the figures of radial velocity profile in this paper are chosen so as to maximize the cosine part of the intensity of the primary harmonic.

3.2 Effects of Energetic Ion Orbit Width

We have carried out simulations for various energetic ion orbit widths. Since the energetic ion orbit width is roughly given by $q\rho_{h\|}$, we solved the extended Grad-Shafranov equation for various $\rho_{h\|}/a$ for the initial conditions of simulation. The Alfvén velocity, major and minor radii, energetic ion and bulk beta values, and energetic ion distribution in the velocity space are kept constant for all of the equilibria. For $\rho_{h\|}/a = 0.02$, no unstable mode was observed. The frequencies are roughly constant for all the cases. The peak locations and the radial widths of the unstable mode spatial profile are shown in Fig. 3. The radial width of the spatial profile is defined by the region where the total intensity of $m/n = 2/1$ harmonic of radial velocity v_r is greater than 10% of the peak value. For the greater $\rho_{h\|}/a$ values, the peak location moves radially outward and the radial width is broadened. The radial width of the mode spatial profile

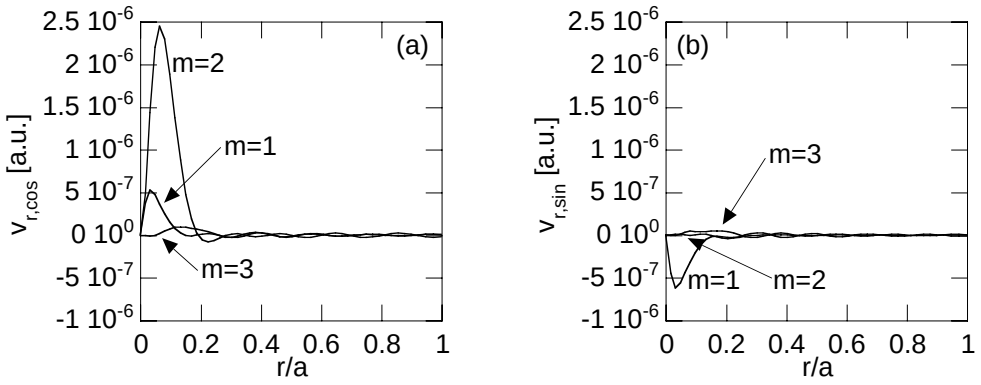

FIG. 4. Spatial profiles of (a) cosine part and (b) sine part of the unstable mode radial velocity v_r harmonics for $\rho_{h\|}/a = 0.033$. The toroidal mode number of all the harmonics is $n = 1$.

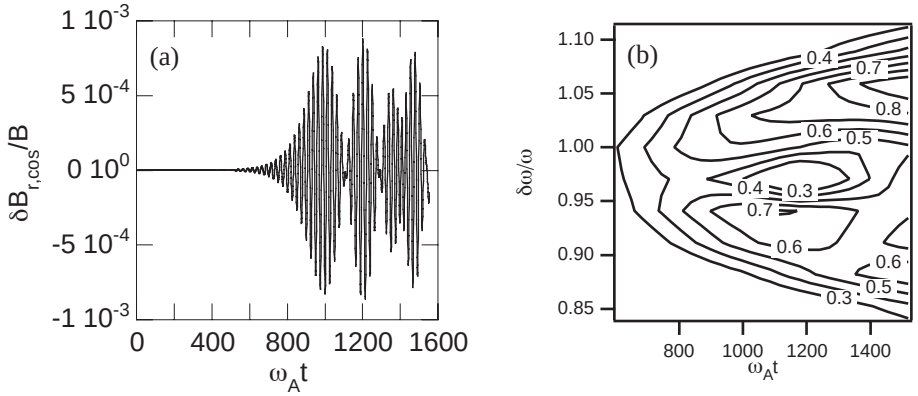

FIG. 5. Time evolution of (a) cosine part and (b) frequency spectrum of the radial magnetic field with the mode number $m/n = 2/1$ for the reduced energetic ion distribution. A Gaussian time window $\exp[-(t-t_0)^2/(400\omega_A^{-1})^2]$ is used for the frequency spectrum analysis.

differs by a factor 3 between the smallest and largest orbit width. The energetic ion orbit width has significant effects on the mode spatial profile. The spatial profile of the unstable mode for the smallest orbit width with $\rho_{h\|}/a = 0.033$ is shown in Fig. 4. The spatial profile is extremely localized near the plasma center. The sine component of $m/n = 2/1$ harmonic of radial velocity v_r is negligibly small compared to the cosine part. The radial width of the unstable mode shown in Fig. 4 gives an upper limit of the radial width of a purely MHD eigenmode if it does exist. We have carried out simulations for various energetic ion pressures and found that the energetic ion pressure also has significant effects on the mode spatial profile.

The spatial width of the unstable mode with the smallest orbit width gives an upper limit of the spatial width which the MHD effects alone can induce. For the experimental condition of the JT-60U plasma, the energetic ions broaden the spatial profile of the unstable mode by a factor of 3 compared with the smallest orbit width case. The major part of the spatial profile of the unstable mode is induced by the energetic ions. It is concluded that the unstable mode is primarily induced by the energetic particles and the name "nonlocal EPM" [8] can be justified.

4. Nonlinear Evolution of the Nonlocal EPM

In this section we report the results of the nonlinear simulation using the MEGA code. The viscosity and resistivity used in the simulation are $2 \times 10^{-5} v_A R_0$ and $2 \times 10^{-5} \mu_0 v_A R_0$,

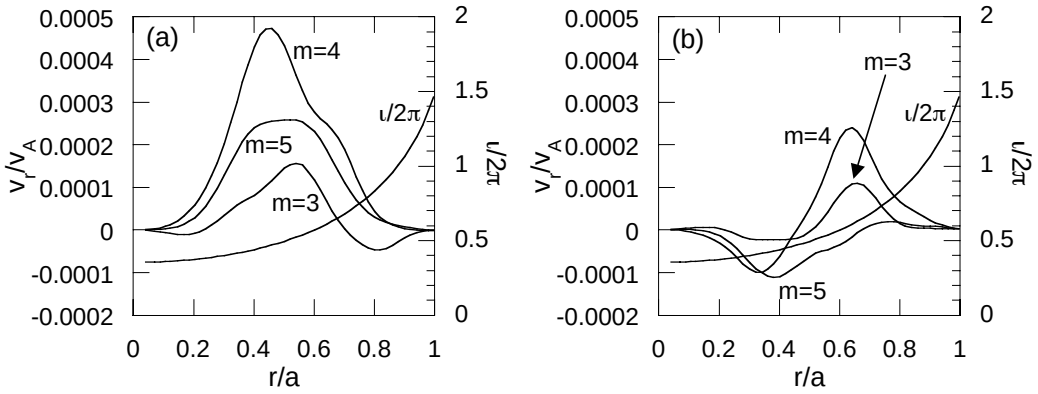

FIG. 6. Spatial profile of (a) cosine part and (b) sine part of radial velocity of the TAE in the LHD-like plasma with the toroidal mode number $n = 2$ and the rotational transform profile.

respectively, where v_A is the Alfvén velocity at the magnetic axis and μ_0 the vacuum magnetic permeability. We consider a reduced energetic ion pressure profile because in the experiments redistributions and losses of energetic ions take place due to the fast FS mode and the ALE with time intervals much shorter than the slowing down time. The classical distribution gives an overestimate of the energetic ion pressure profile. Simulations which take into account the MHD activity, NNB injection, and collisions are needed to obtain self-consistent energetic ion distributions. It is, however, computationally too demanding and beyond the scope of this paper. We carried out a run where the energetic ion pressure is reduced to 2/5 while the spatial profile is the same as the classical distribution which is shown in Fig. 1(a). Figure 5(a) shows the time evolution of cosine part of $m/n = 2/1$ harmonic of the radial magnetic field. An oscillation in amplitude takes place after saturation. The saturation level of the magnetic field fluctuation is $\delta B/B \sim 8 \times 10^{-4}$. It is found that the frequency shifts upward by 9% ($\sim$5kHz) and downwards by 9% ($\sim$5kHz) of the linear frequency in 10^3 Alfvén time ($\sim$0.8ms). This frequency shifts are close to those of the fast FS mode.

The frequency upshift and downshift due to the spontaneous hole-clump pair creation in a phase space was found by simulating a reduced kinetic equation when the linear damping rate (γ_d) is greater than 0.4 of the linear growth rate without damping (γ_L) [9, 10]. The theory predicts frequency shifts $\delta\omega = 0.44\gamma_L(\gamma_d t)^{1/2}$. This gives $\delta\omega \sim 0.03\omega_A$ in 10^3 Alfvén time. This corresponds to 6 kHz . The rate of the frequency shifts in the simulation results is consistent with what the theory predicts.

5. Toroidicity-induced Alfvén Eigenmode in an LHD-like Plasma

The MEGA code has been successfully extended to simulate helical plasmas using the helical coordinate system which is employed in the MHD equilibrium code, HINT [29]. The relation between the helical coordinates (u^1, u^2, u^3) and the cylindrical coordinates (R, φ, z) is

$$R = R_0 + u^1 \cos(hMu^3) + u^2 \sin(hMu^3), \quad (8)$$

$$\varphi = -u^3, \quad (9)$$

$$z = -[u^1 \sin(hMu^3) - u^2 \cos(hMu^3)], \quad (10)$$

where we take for the LHD plasmas $M = 10$ and $h = -0.5$. The physics model and the numerical algorithm are the same as described in section 2.The vector calculations must be done using the covariant and contravariant vectors, because the helical coordinates are not orthogonal. The code is benchmarked for the MHD force balance and a test particle orbit in an MHD equilibrium calculated using the HINT code. In the simulation run reported in this paper, the

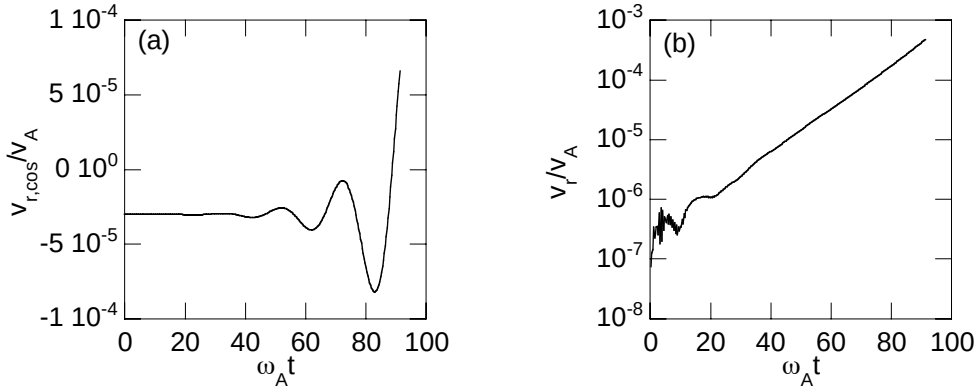

FIG.7 Time evolution of (a) cosine part and (b) amplitude of the radial velocity with the mode number $m/n = 4/2$.

numbers of grid points used are (91, 115, 1000) for (u^1, u^2, u^3) and the number of marker particles used is 4×10^6. A Boozer coordinate system was constructed to analyze the simulation data. The major and minor radii are $R_0 = 3.73$m and $a = 0.89$m, respectively. The magnetic field intensity at the magnetic axis is 0.5T and the Alfvén velocity divided by the hydrogen Larmor frequency is $v_A/\Omega_i = 4.7 \times 10^{-2}$ m. The velocity distribution of energetic ions is a slowing-down distribution with the maximum velocity of $1.2v_A$. The perpendicular velocity of the energetic ions is neglected. The energetic ion beta value at the plasma center is 2%. A TAE with the toroidal mode number $n = 2$ is destabilized. The spatial profile of the TAE is shown in Fig. 6. The dominant harmonics are $m/n = 4, 5/2$. The time evolutions of the cosine part and the absolute value of a radial velocity harmonic with the poloidal and toroidal mode numbers $m/n = 4/2$ are shown in Fig. 7. It can be seen that the real frequency of the TAE is $\omega/\omega_A \sim 0.29$ and the growth rate is $\gamma/\omega_A \sim 0.081$. The frequency and the location of the TAE are consistent with the theory [6].

Acknowledgments

The authors would like to thank Drs. M. Okamoto, Y. Kusama, and T. Ozeki for valuable advice and continuous encouragement. The authors ackonwledge helpful discussions with Dr. H. Miura on the Fourier analysis method in the Boozer coordinates for helical plasmas. Numerical computations were performed at the Man-Machine Interactive System for Simulation (MISSION) of National Institute for Fusion Science. This work was partially supported by Grants-in-Aid for Scientific Research of the Japan Society for the Promotion of Science (Nos. 14780396, 16560728).

References

[1] Y. Kusama, G. J. Kramer, H. Kimura *et al.*, Nucl. Fusion **39**, 1837 (1999).

[2] G. J. Kramer, M. Iwase, Y. Kusama *et al.*, Nucl. Fusion **40**, 1383 (2000).

[3] K. Shinohara, Y. Kusama, M. Takechi *et al.*, Nucl. Fusion **41**, 603 (2001).

[4] K. Shinohara, M. Takechi, M. Ishikawa *et al.*, Nucl. Fusion **42**, 942 (2002).

[5] C. Z. Cheng, L. Chen, and M. S. Chance, Ann. Phys. (N.Y.) **161**, 21 (1985).

[6] C. Z. Cheng and M. S. Chance, Phys. Fluids **29**, 3659 (1986).

[7] Y. Todo and T. Sato, Phys. Plasmas **5**, 1321 (1998).

[8] Y. Todo, K. Shinohara, M. Takechi, and M. Ishikawa, J. Plasma Fusion Res. **79**, 1107 (2003), http://jspf.nifs.ac.jp/Journal/2003.html.

[9] H. L. Berk, B. N. Breizman, and N. V. Petviashvili, Phys. Lett. A **234**, 213 (1997); **238**, 408(E) (1998).

[10] H. L. Berk, B. N. Breizman, J. Candy, M. Pekker, and N. V. Petviashvili, Phys.Plasmas **6**, 3102 (1999).

[11] L. Chen, Phys. Plasmas **1**, 1519 (1994).

[12] C. Z. Cheng, N. N. Gorelenkov, and C. T. Hsu, Nucl. Fusion **35**, 1639 (1995).

[13] H. L. Berk, D. N. Borba, B. N. Breizman, S. D. Pinches, and S. E. Sharapov, Phys. Rev. Lett. **87**, 185002 (2001).

[14] F. Zonca, S. Briguglio, L. Chen, S. Dettrick, G. Fogaccia, D. Testa, and G. Vlad, Phys. Plasmas **9**, 4939 (2002).

[15] K. Appert, R. Gruber, F. Troyon, and J. Vaclavik, Plasma Physics **24**, 1147 (1982).

[16] A. Fukuyama and T. Akutsu, in proceedings of the 19th IAEA Fusion Energy Conference, 2002, Lyon (IAEA, 2003), TH/P3-14.

[17] B. N. Breizman, H. L. Berk, M. S. Pekker, S. D. Pinches, and S. E. Sharapov, Phys. Plasmas **10**, 3649 (2003).

[18] Y. Todo, K. Shinohara, M. Takechi, and M. Ishikawa,“Nonlocal energetic particle mode in a JT-60U plasma”, to appear in Phys. Plasmas.

[19] W. Park, S. Parker, H. Biglari, M. Chance, L. Chen, C. Z. Cheng, T. S. Hahm, W. W. Lee, R. Kulsrud, D. Monticello, L. Sugiyama, and R. White, Phys. Fluids B **4**, 2033 (1992).

[20] Y. Todo, T. Sato, K. Watanabe, T. H. Watanabe, and R. Horiuchi, Phys. Plasmas **2**, 2711 (1995).

[21] A. M. Dimits and W. W. Lee, J. Comput. Phys. **107**, 309 (1993).

[22] S. E. Parker and W. W. Lee, Phys. Fluids B **5**, 77 (1993).

[23] A. Aydemir, Phys. Plasmas **1**, 822 (1994).

[24] E. V. Belova, N. N. Gorelenkov, and C. Z. Cheng, Phys. Plasmas **10**, 3240 (2003).

[25] R. Nazikian, G. Y. Fu, S. H. Batha et al., Phys. Rev. Lett. **78**, 2976 (1997).

[26] G. Y. Fu, R. Nazikian, R. Budny, and Z. Chang, Phys. Plasmas **5**, 4284 (1998).

[27] Y. Chen, R. B. White, G. Y. Fu, and R. Nazikian, Phys. Plasmas **6**, 226 (1999).

[28] K. Tani, M. Azumi, H. Kishimoto, and S. Tamura, J. Phys. Soc. Jpn **50**, 1726 (1981).

[29] K. Harafuji, T. Hayashi, and T. Sato, J. Comput. Phys. **81**, 169 (1989).